

## Solar Cycle 23 in Coronal Bright Points

Isroil Sattarov · Alexei A. Pevtsov · Nina V. Karachik ·  
Chori T. Sherdanov · A.M. Tillaboev

Received: 13 May 2009 / Accepted: 23 January 2010 / Published online: 13 February 2010  
© Springer Science+Business Media B.V. 2010

**Abstract** We describe an automatic routine to identify coronal bright points (CBPs) and apply this routine to SOHO/EIT observations taken in the 195 Å spectral range during solar cycle 23. We examine the total number of CBPs and its change in the course of this solar cycle. Unlike some other recent studies, we do find a modest  $\approx 30\%$  decrease in the number of CBPs associated with maximum of sunspot activity. Using the maximum brightness of CBPs as a criterion, we separate them on two categories: dim CBPs, associated with areas of a quiet Sun, and bright CBPs, associated with an active Sun. We find that the number of dim coronal bright points decreases at the maximum of sunspot cycle, while the number of bright CBPs increases. The latitudinal distributions suggest that dim CBPs are distributed uniformly over the solar disk. Active Sun CBPs exhibit a well-defined two-hump latitudinal profile suggestive of enhanced production of this type of CBPs in sunspot activity belts. Finally, we investigate the relative role of two mechanisms in cycle variations of CBP number, and conclude that a change in fraction of solar surface occupied by the quiet Sun's magnetic field is the primary cause, with the visibility effect playing a secondary role.

**Keywords** Instrumentation and data management · Solar corona, structures · Solar cycle

---

Solar Image Processing and Analysis  
Guest Editors: J. Ireland and C.A. Young

I. Sattarov · A.M. Tillaboev  
Tashkent State Pedagogical University, 103 Yusuf Khos Khojib Street, Tashkent 700100, Uzbekistan

I. Sattarov  
e-mail: [isattar@astrin.uzsci.net](mailto:isattar@astrin.uzsci.net)

A.A. Pevtsov (✉) · N.V. Karachik  
National Solar Observatory, PO Box 62, Sunspot, NM 88349, USA  
e-mail: [apectsov@nso.edu](mailto:apectsov@nso.edu)

N.V. Karachik  
e-mail: [nkarachi@nso.edu](mailto:nkarachi@nso.edu)

C.T. Sherdanov  
Astronomical Institute AS of Uzbekistan, 33 Astronomical str., Tashkent 100052, Uzbekistan  
e-mail: [chori@astrin.uzsci.net](mailto:chori@astrin.uzsci.net)

## 1. Introduction

Historically, the term X-ray bright points (XBPs) was used to describe compact coronal brightenings observed in X-rays. Here, we adopt a more general term, coronal bright points (CBPs), as first suggested by Webb *et al.* (1993). CBPs were discovered on first X-ray images of the Sun taken from sounding rockets. Later, their properties were extensively studied using observations from the Skylab and the sounding rocket experiments. These early studies had indicated several major properties of these coronal features: *i*) the existence of two types of CBPs (Golub, Krieger, and Vaiana, 1975), *ii*) their association with cancelling magnetic bipoles (Harvey-Angle, 1993), *iii*) a cycle variation of the number of CBPs (Davis, Golub, and Krieger, 1977; Golub, Davis, and Krieger, 1979) and *iv*) enhancement of the CBP number near sunspot activity complexes (Golub, Krieger, and Vaiana, 1975).

Using a limited data set of daily full disk magnetograms, Webb *et al.* (1993) and Harvey-Angle (1993) studied magnetic counterparts of CBPs. They found that a majority of these coronal structures were associated with canceling (converging and disappearing) magnetic bipoles. About 30% of the CBPs was found to be related to ephemeral active regions.

Golub, Krieger, and Vaiana (1975) studied latitudinal and longitudinal distribution of X-ray bright points during a single solar rotation and concluded that the latitudinal distribution of CBPs has two components: one represents uniform distribution of CBPs over solar surface, and the other characterizes CBPs formed in sunspot activity belts. Statistical study of X-ray bright points (Sattarov *et al.*, 2002) using *Yohkoh* soft X-ray telescope data (SXT, Tsuneta *et al.*, 1991) showed a clear presence of the Spörer's butterfly distribution in XBPs similar to solar active regions. Observations with the Extreme ultraviolet Imaging Telescope (EIT) on board of the *Solar and Heliospheric Observatory* (SOHO) also showed enhancement of CBPs in sunspot activity belts (McIntosh and Gurman, 2005). In respect to the longitudinal distribution, Golub, Krieger, and Vaiana (1975) noted that the CBP number is enhanced at longitudes near sunspot complexes of activity. This was later confirmed by Sattarov *et al.* (2005a), who had described enhancement in the CBP number near the location of sunspot activity complexes.

Davis, Golub, and Krieger (1977) had found that the number of CBPs varies inversely with sunspot cycle. Following this discovery, Golub, Davis, and Krieger (1979) had suggested the existence of a secondary cycle of magnetic activity running in opposite phase to the sunspot cycle. However, later, Hara and Nakakubo-Morimoto (2000) found that the variation in the number of CBPs might be explained by the visibility effect (see, also, Hara and Nakakubo-Morimoto, 2003). The visibility effect includes two components. First, the overall brightness of a high temperature corona may be significantly affected by the presence of bright active regions (*e.g.*, Pevtsov and Acton, 2001), and the enhanced brightness of the corona may hinder identification of dimmer CBPs. Second, areas close to active regions could be "occulted" by a canopy of bright active region corona. In both cases, the visibility effect implies that the bright points are still present, but they cannot be identified because of the enhanced background coronal brightness in their vicinity. Sattarov *et al.* (2002) drew conclusions similar to Hara and Nakakubo-Morimoto (2000) about the role of visibility effect on the basis of the lack of solar-cycle variation in a number of photospheric bipoles. The number of bright points in data due to Sattarov *et al.* (2002) showed clear cycle variations, while the number of magnetic bipoles with a particular size and separation did not show such variations. Assuming that the fraction of magnetic bipoles associated with CBPs does not change with solar cycle, Sattarov *et al.* (2002) have concluded that the cycle variation of CBPs is apparent, and it is probably caused by changes in overall brightness of the solar corona as suggested by Hara and Nakakubo-Morimoto (2000).

The advancement of computational capabilities and the open-data policy led to the development of several methods for automatic identification of coronal bright points. The details of these methods can be found elsewhere (*e.g.*, Hara and Nakakubo-Morimoto, 2003; Sattarov *et al.*, 2005a, 2005b; McIntosh and Gurman, 2005; Karachik, Pevtsov, and Sattarov, 2006). Using automatic algorithms and objective criteria enables massive statistical studies of coronal bright points previously unavailable. As the first step, it is natural to re-examine previously discovered tendencies and properties of CBPs using significantly larger and more uniform data sets. In this paper, we use the automatic procedure developed by us to identify the coronal bright points over the period of the complete solar cycle 23, 1996–2008. We apply this method to SOHO/EIT 195 Å data to study the statistical distribution of CBPs with the solar cycle. To investigate the significance of the visibility effect, we analyze background intensity around CBPs and its change with sunspot activity. We compare background intensity and CBP number at equator, activity belts, and high latitudes, where the consequences of the visibility effect should be different. In addition to cycle variations in CBPs, we study their latitudinal distributions. The rest of the paper is organized as follows. In Section 2, we describe our data set and provide a detailed description of our automatic procedure to identify coronal bright points. In Section 3, we review our major findings, in Section 4 we discuss the relative role of the visibility effect and provide an alternative explanation for cycle variation of the coronal bright points, and in Section 5, we summarize our findings.

## 2. Data Sets and Automatic Procedure for Identification of CBPs

In this work we use full disk images observed by the Extreme-ultraviolet Imaging Telescope (EIT, Delaboudinière *et al.*, 1995) on board of SOHO. We utilize EIT full disk synoptic data with spatial resolution of 2.64 arcsec per pixel and six hours cadence observed in 195 Å from 1996–2008. The data are calibrated following the standard EIT data reduction routine. The calibration routine normalizes the exposure time and takes into account change in response of CCD camera over the time of mission.

To identify coronal bright points, we employ the automatic procedure developed by us (first presented in June 2004 at the IAU Symposium 223, see also Sattarov *et al.*, 2005a, 2005b). The procedure was modified by Karachik, Pevtsov, and Sattarov (2006) to improve the categorization of CBPs either as previously existing or newly emerged bright points.

We implement the following steps in the CBP identification:

- Subtraction of large scale variations in the corona.
- Exclusion of compact brightenings above active regions from the CBP search.
- Identification of potential CBPs.
- Analysis of shape and length of potential CBPs to exclude hot pixels, cosmic ray streaks, and loop-like features not associated with active regions.

The following sections provide a detailed description of each step.

### 2.1. Step 1: Subtraction of Large Scale Variations in the Corona

The X-ray and Extreme Ultra-Violet (EUV) corona observed on solar disk exhibits variations in brightness on different spatial scales. For example, the areas of coronal holes and filament channels are darker, while the areas of strong closed magnetic fields have an enhanced brightness. Thus, using a fixed intensity threshold (as was done, for example, in Zhang, Kundu, and White, 2001) will only work satisfactorily on images with a low sunspot activity.

We have adopted an alternative approach and identify CBPs relative to brightness of background corona near potential CBP. To remove large-scale intensity variations, we subtracted a median-smoothed image from the original full disk data. The size of the median filter was determined by comparing the location and number of CBPs found on the difference image with CBPs selected using the fixed intensity threshold applied to selected images with no active regions. This procedure was repeated on several EIT images taken during 1996–1997 when sunspot activity was low. The validity of the median filter found using the 1996–1997 data was tested on selected full disk images with various levels of coronal activity (with active regions present on the disk). In the latter case, coronal bright points identified after subtraction of images smoothed by median filter were compared with a manual identification of CBPs.

This process had yielded a very similar size for the median filter for different images, and finally a median filter with 30 pixels in width was adopted as the standard median filter for our CBP selection routine. Figure 1 shows an example of an EIT image and identification of CBPs after applying the median filter.

## 2.2. Step 2: Exclusion of Compact Brightenings Above Active Regions from the CBP Search

Subtracting a median-filtered image from the original image improves the identification of bright points. Unfortunately, in some cases it might also lead to false identifications of bright portions of active region (AR) loops as coronal bright points. To prevent these false identifications, we excluded areas of active regions from search for CBPs. Active regions are excluded based on their brightness and total area. Using original image, the routine identifies potential active regions as areas whose brightness exceeds AR threshold. This threshold was fixed at the level of 600 Data Numbers per second ( $\text{DN s}^{-1}$ ) based on a trial-and-error approach on many images. In selecting this threshold, we used data with various levels of sunspot activity (both during a minimum and maximum of the activity cycle). In part, the threshold selection was made to optimize selection of CBPs and minimize false-positives such as bright loop-tops situated inside of active regions.

Next, potential active regions were verified based on their total continuous area (area within a closed contour). If the total area of a potential active region had exceeded the area of a circle with a radius of 25 arcsec (maximum radius of CBP), the area was labeled as an active region, and all potential bright points identified within the area were excluded from consideration. Bright areas that were not classified as active regions remained as valid locations for potential bright points. The above two-step approach in identifying active regions allows us to avoid the exclusion of bright areas in the solar corona not associated with active regions such as, for example, areas of relatively bright but diffuse corona. A size threshold for active regions was adopted from the manual survey of CBPs by Longcope *et al.* (2001).

## 2.3. Step 3: Identification of Potential CBPs

After subtracting the median-average, we computed the average brightness  $I_{\text{avg}}$  and its standard deviation  $\sigma$  using the difference image. In computing  $I_{\text{avg}}$ , all pixels corresponding to potential bright points are excluded as explained below.

A brightness level ( $I_{\text{thresh}}$ ) that separates “quiet Sun” and “active” corona was found iteratively by exclusion of the brightest pixels and using the remaining pixels to compute  $I_{\text{avg}}$  until the condition  $I_{\text{avg}} \approx 0$  was satisfied.

After determining  $I_{\text{avg}}$  and  $\sigma$ , we selected all closed contours with intensity exceeding  $I_{\text{avg}} + \sigma$  for further examination as potential bright points. Next, we selected a small sub-image around each potential bright point and computed the center of gravity of the potential

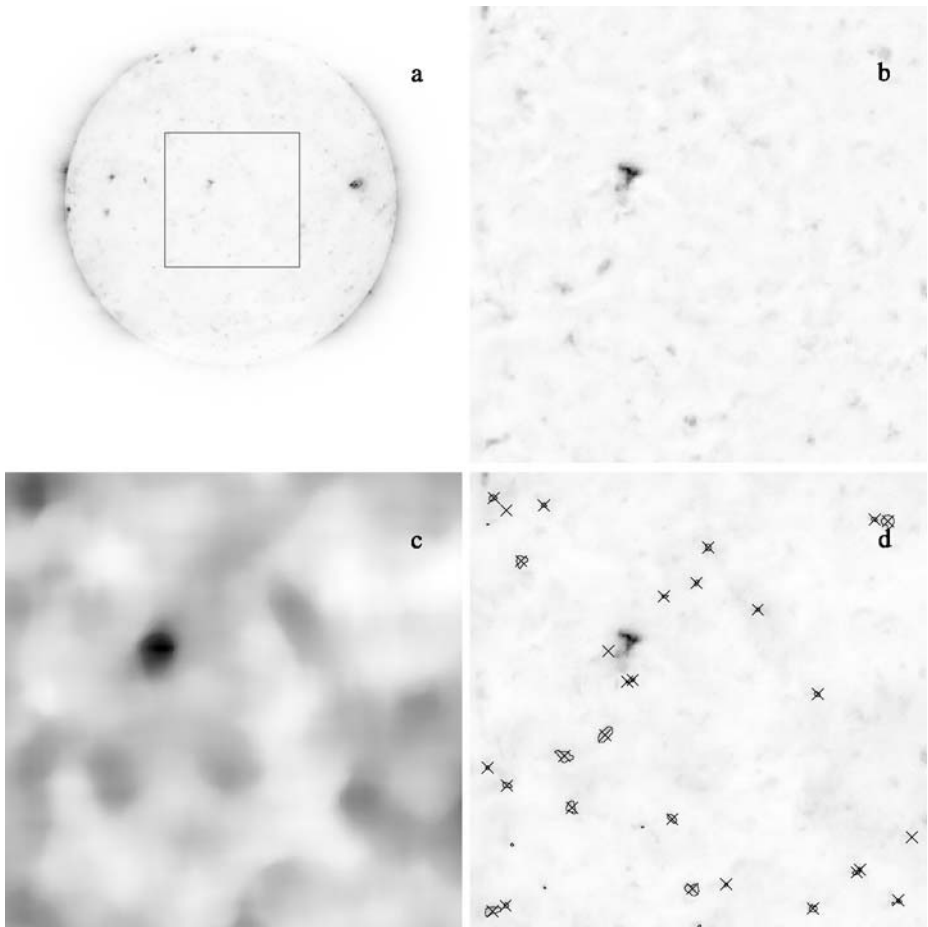


**Figure 1** EIT full disk image (reversed colors) taken on 2 April 1996. For demonstration purposes, panel (b) shows an area of 300 pixels by 300 pixels near disk center, the same area smoothed by median filter (c), and coronal bright points selected using the fixed intensity threshold (contours) and by our method (crosses). Note that the brightest feature on panel (d) did not pass the “active region” threshold and, hence, is not selected as a CBP.

bright point ( $C_g$ ) and its radius ( $R_{cbp}$ ).  $R_{cbp}$  is the maximum distance between  $C_g$  and the contour outlining the CBP boundary. Each selected sub-image is a square centered at  $C_g$  with sides  $2 \times R_{cbp}$  in size, but not less than 26 pixels. Using these sub-images we further refined our definition of potential CBP as a region of sub-image with an area of more than one pixel and an intensity above  $I_{subavg} + 2\sigma_{sub}$ , where  $I_{subavg}$  and  $\sigma_{sub}$  are the average and its standard deviation of intensity of the sub-image containing the potential bright point.

#### 2.4. Step 4: Analysis of Shape and Length of Potential CBPs

The final selection of coronal bright points was refined using several additional criteria: total area of potential CBPs, their shape, and angular distance from the disk center ( $\rho < 0.95R_{Sun}$ ). For example, we did not count as CBPs features whose radius is smaller than 2 Mm (potential hot pixels) or larger than 20 Mm (potential ephemeral active regions). We

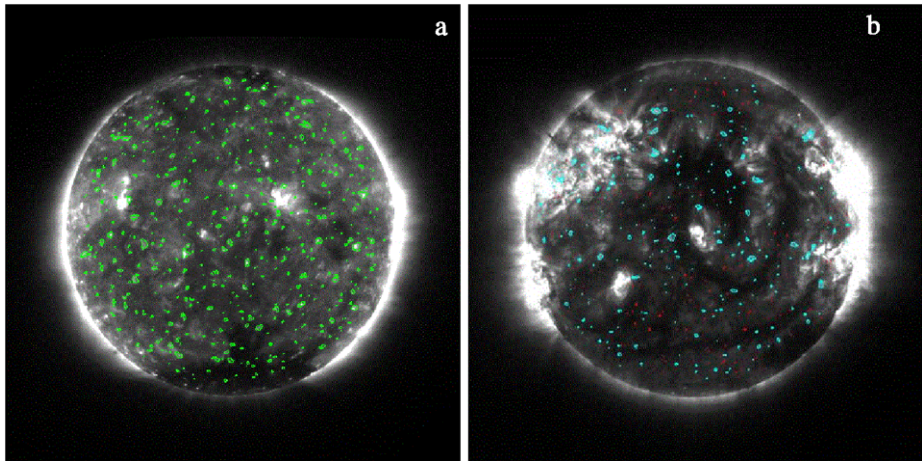


**Figure 2** EIT full disk images for two periods of higher sunspot activity in the years (a) 2000 and (b) 2001. Color contours show CBPs identified by our program.

also excluded highly elongated and crescent-like structures that may correspond to bright portions of isolated long coronal loops. If the maximum radius of potential CBP was five times larger than its minimum radius, the feature was excluded because of its excessive elongation. Similarly, when the geometric center of a potential CBP was located outside of closed contour outlining CBP, the feature was excluded because of its crescent-like or irregular shape. The stated limits of the maximum size of the potential bright point were adopted from the manual survey by Longcope *et al.* (2001). The above size-limits were supported by the distribution of sizes of CBPs in Sattarov *et al.* (2005c).

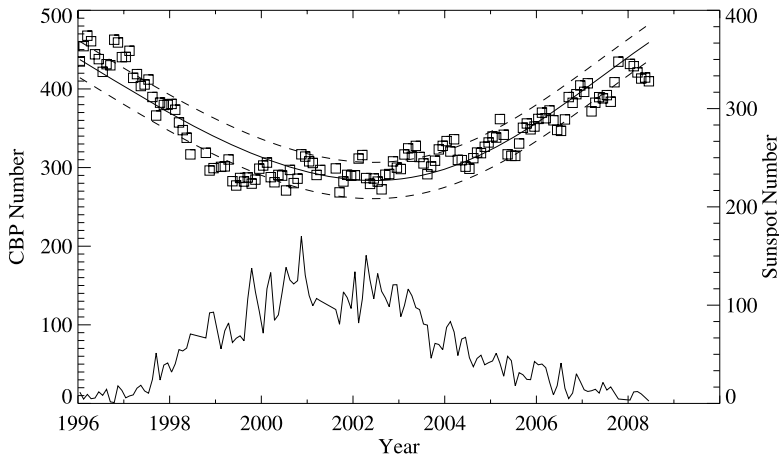
According to current knowledge about the coronal bright points, many if not all of these features may, in fact, be associated with small loops connecting opposite polarity footpoints. Thus, exclusion of elongated and crescent-like features because of their potential relation with the coronal loops might appear counter-intuitive. However, it should be emphasized that we only excluded such features when they were related to long loops, which in our opinion, do not fit the traditional definition of the coronal bright point as a compact feature.

Figure 2 provides two examples of CBP selection during periods of higher sunspot activity as compared with the example shown on Figure 1.

### 3. Coronal Bright Points and Solar Cycle

Figure 3 shows the monthly-averaged number of coronal bright points per solar visible disk during 1996–2008. The CBP number exhibits a clear decrease associated with a maximum of the sunspot activity cycle; this decrease is at odds with some previous studies of coronal bright points. For example, data due to McIntosh and Gurman (2005) show an unexplained jump in CBP number in early 1998 as well as a slight increase towards 2002, a year on the sunspot cycle maximum. On the other hand, Hara and Nakakubo-Morimoto (2003) have found a small ( $\approx 20\%$ ) increase in the total number of X-ray bright points associated with the minimum of solar cycle 22.

The total number of CBPs in our data set is about 280–450 per image, which exceeds the number of bright points found in McIntosh and Gurman (2005) for Fe XIII 195 Å (230–300



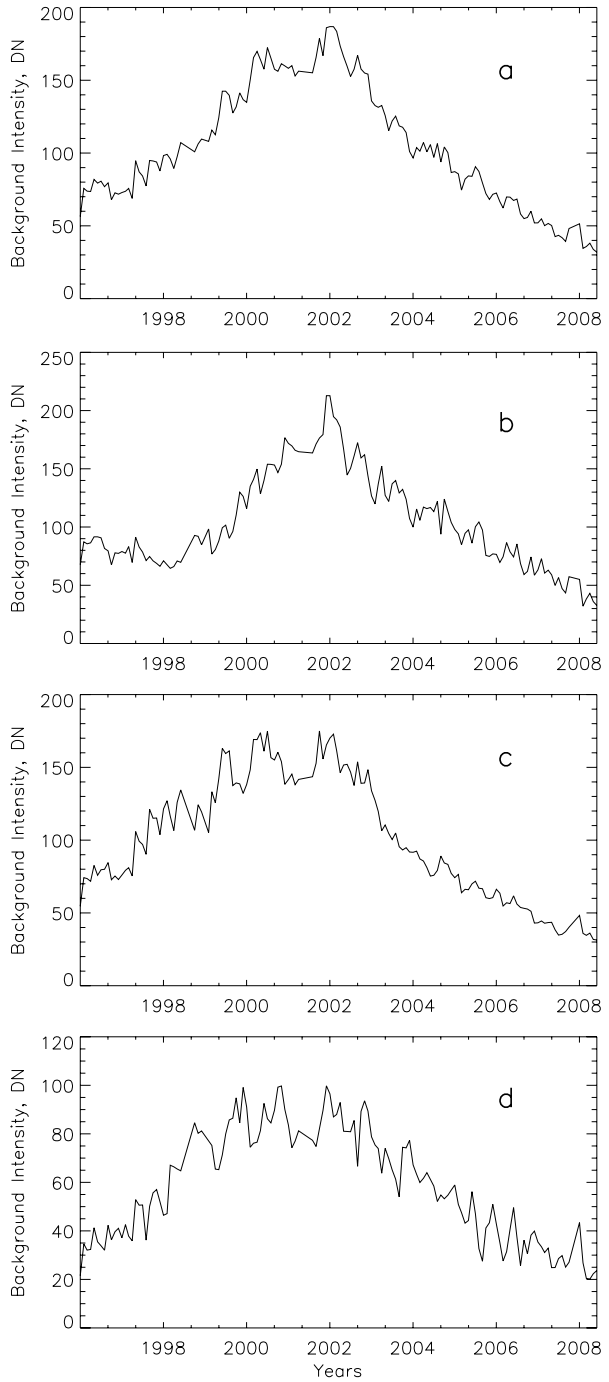
**Figure 3** Cycle variation of coronal bright points (monthly-averaged, squares) and monthly sunspot number (lower curve). The solid line surrounded by two dashed lines represents the change in CBP number with solar cycle derived on the basis of a Gaussian fit to the distribution of dim and bright CBPs shown in Figure 5. The two dashed lines represent one sigma standard deviation of the fit shown by the solid line.

per image). Assuming a uniform distribution of CBPs over the solar surface, the number of CBPs found in McIntosh and Gurman (2005) translates to a density of coronal bright points of  $0.8 - 1.0 \times 10^{-4} \text{ Mm}^{-2}$ . Our data yield a density of coronal bright points of about  $0.9 - 1.5 \times 10^{-4} \text{ Mm}^{-2}$ . For comparison, Longcope *et al.* (2001) had estimated a density of CBPs as high as  $1.3 \times 10^{-4} \text{ Mm}^{-2}$  and Golub, Krieger, and Vaiana (1976) found  $0.6 - 2.0 \times 10^{-4} \text{ Mm}^{-2}$ . Hara and Nakakubo-Morimoto (2003) had reported the density of X-ray bright points to be  $0.2 - 0.7 \times 10^{-4} \text{ Mm}^{-2}$ . According to Zhang, Kundu, and White (2001) the XBP number is about 3–4 times smaller than the number of CBPs observed by EIT. With this correction, the XBP number density found in Hara and Nakakubo-Morimoto (2003) is in general agreement with Longcope *et al.* (2001) and Golub, Krieger, and Vaiana (1976). The density of coronal bright points found by us is in agreement with Longcope *et al.* (2001) and Golub, Krieger, and Vaiana (1976). A slight disagreement between the number of bright points with McIntosh and Gurman (2005) can be attributed to a difference in size of CBPs identified by the two procedures. Sattarov *et al.* (2005c) have given an example of a distribution of CBPs by their size. In that example, the total number of CBPs was about 460 per image, and there were only about 200 CBPs with area larger than 20 pixels.

The CBP data shown in Figure 3 exclude the smallest CBPs (2 pixels in total area) identified by our routine. The data set that includes these smallest CBPs yields about 400–600 CBPs per image. Although the solar-cycle variation is still present (albeit at a reduced amplitude of about 20% change between 1996 and 2002), the data show significantly larger scatter and “jumps” in CBP number. We see the latter as an indication that the EIT spatial resolution is only marginally sufficient to resolve these smallest CBPs.

As part of our CBP identification procedure, we have analyzed the average brightness of the corona in the vicinity of each CBP as well as the maximum brightness of the CBPs themselves. Figure 4 shows the monthly-averaged brightness of the background in sub-images that were used in the final CBP identification ( $I_{\text{subavg}}$ , see Section 2.3). Not surprisingly, the brightness of the background corona varies with sunspot activity. The increase in background brightness near the sunspot maximum is evident in areas near the equator, mid latitudes (activity belts), and high latitudes (outside activity belts), and in our opinion,

**Figure 4** Cycle variation of background intensity for: (a) full disk, (b) equatorial region (latitudinal range  $0 \pm 5$  degrees), (c) active region belts ( $+20 \pm 5$  degrees and  $-20 \pm 5$  degrees), and (d) high latitudes ( $+50 \pm 5$  degrees and  $-50 \pm 5$  degrees).





it is the direct effect of bright active regions, whose presence may increase the brightness of a diffuse corona even at a significant distance away from an active region (e.g., Pevtsov and Acton, 2001). At the rising phase of cycle 23, when the decaying fields of sunspots of cycle 22 were still present near the equator, we see an enhanced coronal brightness both at mid-latitudes (Figure 4c) and near the equator (Figure 4b). As the cycle progresses and the sunspot activity drifts to low latitudes, we see a sharper decrease in coronal brightness in mid-latitudes and a more gradual decrease near the equator. This behavior supports our interpretation of active regions as the source of an enhanced corona in the vicinity of CBPs.

It is interesting to note that our CBP identification routine appears to be relatively insensitive to changes in the sensitivity of the EIT detectors. For example, a drastic change in quantum efficiency of EIT CCD in 1997–1999 did not result in a significant change in background intensity (see Figure 4) or total number of CBPs (Figure 3). The EIT response graph (<http://umbra.nascom.nasa.gov/eit/EIT.html#RESPONSE>) indicates that between 1996 and 1997, the detector's response for Fe XII 195 Å had decreased by 50%. Despite this drastic change, however, the CBP number remains nearly constant (Figure 3). Between 1999 and 2008, the detector's response had gradually decreased from 80% (of pre-launch value) to about 15%. Contrary to that, however, Figure 3 shows a gradual increase (not decrease) in CBP numbers during same period. To further evaluate the effects of changes in the detector's response, we have conducted the following experiment. We have selected a typical EIT image and reduced its overall intensity by 50%. Because CCD is a linear detector, one should expect that a loss of sensitivity will have a linear effect with respect to the image brightness. The total number of CBPs for this degraded image is only about 10% smaller as compared with the original image. To simulate a non-linear change in the CCD response, we reduced the contrast of our test image by 10%. This resulted in only a minor reduction (about 1%) of the total number of CBPs as compared with the original image. Thus, we believe that a change in the EIT detector's response over the lifetime of the SOHO Mission does not have a significant effect on the CBP number returned by our routine.

In addition to the enhanced background surrounding CBPs, we also see cycle-related variations in maximum brightness of CBPs (not shown). The average CBPs brightness is higher near the maximum of sunspot cycle, and it is lower during the sunspot minima. The enhanced brightness of CBPs near the maximum of a sunspot cycle may indicate the presence of an additional population of bright points associated with stronger fields of active regions. The presence of two populations of CBPs was previously suggested by several researchers (e.g., Golub, Krieger, and Vaiana, 1975; Sattarov *et al.*, 2002; McIntosh and Gurman, 2005).

To investigate the cycle behavior of two CBP populations, we have divided our data set into two categories: dim CBPs with maximum intensity  $I_{\max} \leq 150 \text{ DN s}^{-1}$  and bright CBPs with  $I_{\max} > 150 \text{ DN s}^{-1}$ . The maximum brightness threshold,  $I_{\max} = 150 \text{ DN s}^{-1}$ , was selected on the basis of the variation of  $I_{\max}$  during solar cycle. Thus, for example, in 1996, when the sunspot activity was extremely low, the maximum CBP intensity peaked at about  $150 \text{ DN s}^{-1}$  (see Figure 4 in Sattarov *et al.*, 2005c), which we have adopted as a threshold for dim CBPs.

Figure 5 shows the cycle variation of two types of CBPs. The number of dim CBPs decreases as the sunspot activity grows, while the number of bright CBPs increases. A similar behavior of bright and dim CBPs with solar cycle was previously reported by Hara and Nakakubo-Morimoto (2003). The numbers of dim ( $N_{\text{dim}}$ ) and bright ( $N_{\text{bright}}$ ) CBPs show a linear relation, albeit with a significant scatter. By fitting the first degree polynomial, we found that  $N_{\text{bright}} = (274 \pm 4) - (0.59 \pm 0.02)N_{\text{dim}}$ . The proportionality coefficient being less than unity suggests that an increase in the number of bright CBPs cannot not fully compensate for a decrease in the number of dim CBPs, and hence, one could expect to find a slight

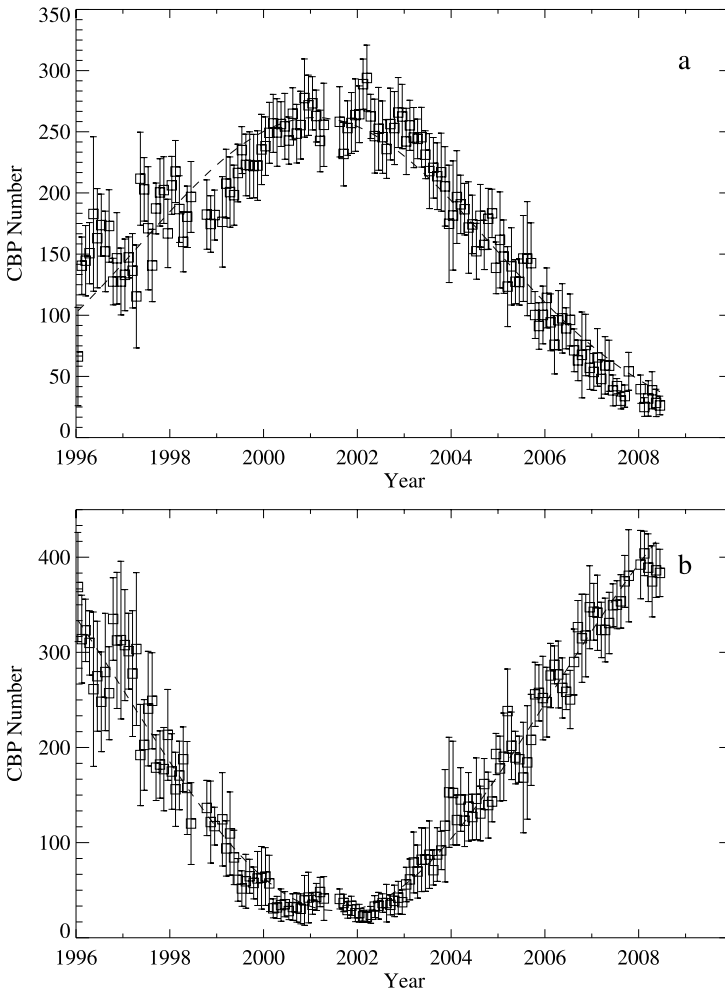


**Figure 5** Cycle variation of (a) “bright” and (b) “dim” CBPs. Open squares with error bars show monthly-averaged numbers of CBPs and their standard deviations. Dashed lines are approximations of two distributions by Gaussian functions.

decrease in the total number of CBPs at/near maximum of sunspot activity. Figure 5 shows a Gaussian fit to distributions of dim and bright CBPs with solar cycle. A sum of these two Gaussian fits is shown as a solid line in Figure 3; two dashed lines correspond to a standard deviation of this fit. The trend suggests a solar-cycle variation of total CBP number at about 30% level. The trend is statistically significant, well exceeding the scatter in data points in Figure 3.

The above relation between number of bright and dim CBPs provides an indirect support to early findings by Webb *et al.* (1993) and Harvey-Angle (1993) who showed that a majority of CBP are associated with canceling bipoles and about one third of them are associated with ephemeral active regions. Assuming that dim CBPs are primarily associated with quiet Sun bipoles, and bright CBPs are “active Sun” features, one can arrive to the conclusion that overall the quiet Sun features well-outnumber the active Sun CBPs. The lat-

**Figure 6** Average latitudinal profiles of number of “dim” CBPs for the years 1996 (solid), 1998 (dashed), and 2002 (dashed-dotted).

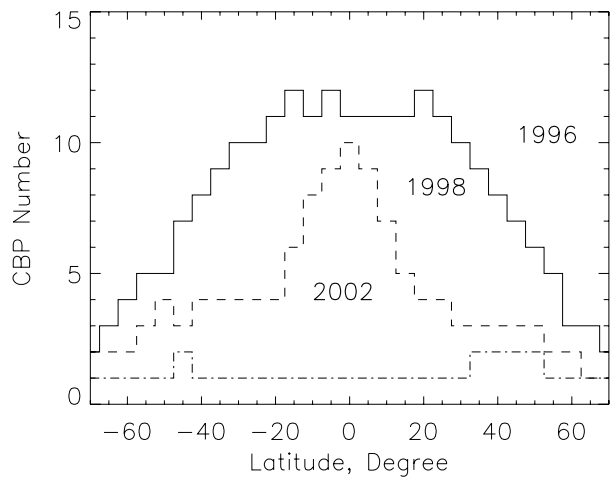
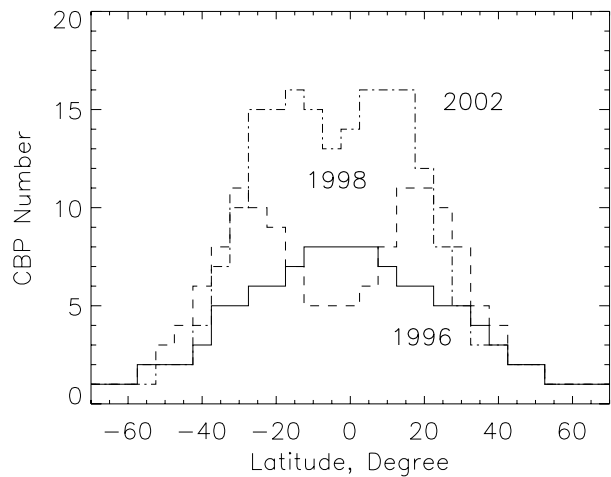


**Figure 7** Average latitudinal profiles of number of “bright” CBPs for the years 1996 (solid), 1998 (dashed), and 2002 (dashed-dotted).



itudinal distribution of two types of CBPs is also different. Dim CBPs are distributed more or less uniformly with solar latitudes (Figure 6, year 1996). The latitudinal profile of bright CBPs exhibits a well-defined hump during years when the sunspot activity is concentrated at mid-latitudes. The latitudinal distribution of bright CBPs shows the migration toward the equator. When the activity belts migrate to the equatorial region, a two-hump pattern in the latitudinal distribution of CBPs disappears (Figure 7). We would like to clarify, however, that our method separates coronal bright points into two types based on their brightness alone. It does not take into account the magnetic properties of CBPs, and therefore, we cannot be certain whatever “quiet Sun” CBPs are indeed associated with canceling bipoles in quiet Sun, nor can we state that “active Sun” CBPs are a product of ephemeral active regions. We plan to investigate such associations in a separate study.

#### 4. Role of Visibility and Other Effects in Cycle Variation of CBP Number

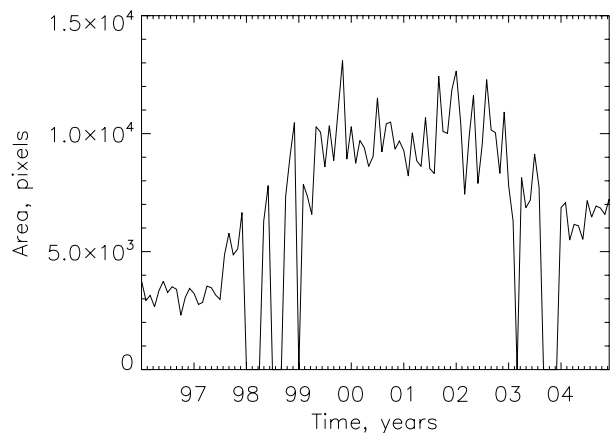
The distribution of CBP number with latitude shown in Figures 6 and 7 suggests a different origin of the two types of CBPs. Bright CBPs are associated with active region activity (for example, an enhanced production of magnetic bipoles around developing/decaying active regions), and dim CBPs are linked to a quiet Sun corona outside of active regions' "sphere of influence". The decrease in number of dim CBPs can be contributed to the visibility effect, as proposed by several researchers (*e.g.*, Hara and Nakakubo-Morimoto, 2000; Sattarov *et al.*, 2002). As a result of enhanced activity, the overall brightness of solar corona increases (Figure 4), which coincides with a decrease in number of CBPs at all latitudes.

On the other hand, the number of dim CBPs may also decrease because the area of quiet Sun that hosts these CBPs decreases as the area occupied by active regions increases. The effect can be seen in the latitudinal distribution of CBPs. For example, in low ( $0 \pm 5$  degrees) and high latitudes ( $50 \pm 5$  degrees), the latitudinal distribution of dim CBPs in 1998 (Figure 6, rising phase of solar cycle) has about the same number of CBPs as the distribution for 1996 (solar minimum). However, the number of dim CBPs is suppressed in mid-latitudes, which approximately corresponds to active region latitudes in Figure 7.

One might argue that if the CBP number changes because of the change in total disk area of an active region, there should be a close relation between the total area of active region excluded by our routine and the number of CBPs. Indeed, we do see a significant cycle variation in the area of active regions in our data (Figure 8). However, the effect could be more complicated than a simple reduction of solar disk area due to the presence of active regions. In fact, a reduction in the area of a quiet Sun can be larger than the area of the active region subtracted by our program. For example, CBP production may be significantly reduced in areas of relatively strong unipolar fields such as plages. However, because of their lower coronal brightness, plages might not be excluded from the CBP search.

Therefore, to better estimate the effect of the changing area occupied by active regions (defined in the broad sense as discussed above) on the number of quiet Sun CBPs, we adopt bright Ca K plages as a proxy for an active region area. Using plages allows for a better estimate of the effects of the changing area of active regions on the total number of CBPs. Ca K plages correspond to areas of relatively strong magnetic fields around active regions; quiet Sun CBPs are not typically present in the close proximity to active regions. In contrast, using bright coronal areas associated with active regions would mix the visibility effect (blockage

**Figure 8** Disk area identified as an active region by our program in the selected subset of data.



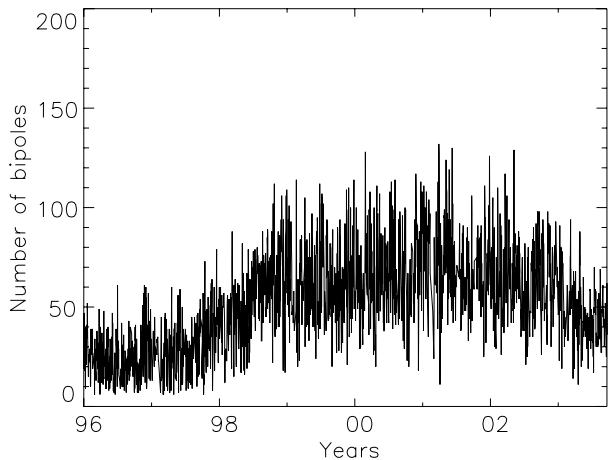
of CBPs by bright active region corona) and the changing area occupied by magnetic field of active regions. Because active regions are excluded from the CBP search, these areas of the Sun are effectively “unavailable” for quiet Sun CBPs. In a solar maximum, the fraction of visible solar disk occupied by Ca K plages can reach about 10% of solar visible disk (e.g., Tlatov, Pevtsov, and Singh, 2009), which approximately corresponds to a circle of radius of 20 (solar) degrees centered at the solar disk center. Taking, for example, the distribution of CBPs for 1996 (Figure 6) and subtracting CBPs from the  $\pm 20$  degrees latitudinal range reduces the total number of CBPs by about 50%. This reduction in CBP number is comparable to the change in total number of the coronal bright points between the solar minimum and maximum (Figure 5a), although it cannot completely explain the change in number of dim CBPs from solar minimum to solar maximum. Thus our estimate agrees with Giovanelli (1982), who found that the area occupied by a mixed polarity field may vary by as much as 80% between solar minimum and maximum.

Thus, the decrease in number of dim CBPs shown in Figure 5b can be explained largely by a decrease in the area of quiet Sun “available” for CBPs, suggesting that the visibility effect may play only a minor role in the cycle variation of coronal bright points. However, to better evaluate the relative contribution of the visibility effect and the effect of the decrease in the fraction of quiet Sun area would require a detailed study of the magnetic properties of areas hosting CBPs. We plan to address this issue in a separate study.

The decreased fraction of solar surface where CBPs can develop is different from the visibility effect. The former implies that magnetic bipoles and coronal bright points are not present in the locations occupied by strong or unipolar fields, while in latter case, CBPs could be present, but they are not detectable because of the presence of a bright corona around or above them. (Although it is not clearly suggested by Hara and Nakakubo-Morimoto (2003), one might interpret their reference to “occultation by active regions” both as a visibility effect and as a decrease in fraction of the solar surface available for CBPs development.)

Sattarov *et al.* (2002) used the lack of variation in the number of magnetic bipoles to support the visibility effect as an explanation for the apparent cycle variation of number of coronal bright points. It will be instructive to repeat their analysis using a higher threshold for the magnetic flux. Using the National Solar Observatory (NSO) at Kitt Peak, full disk longitudinal magnetograms and 50 gauss (G) threshold for magnetic fluxes, we have identified magnetic bipoles from 1996–mid-2003. In this determination, we followed the procedure described by Sattarov *et al.* (2002), except that we used a higher flux threshold to reduce the relative contribution of quiet Sun bipoles with respect to bipoles associated with stronger fields of ephemeral active regions. Figure 9 shows that the number of these bipoles does vary in unison with sunspot cycle. Sattarov *et al.* (2002) used lower (20 G) threshold for magnetic fluxes, and hence, their data may represent a mixture of bipoles associated with dim (quiet Sun) and bright (active region) CBPs. The fact that bipoles with a low flux threshold do not show cycle variation but bipoles with stronger flux do show such a variation suggests that the number of bipoles associated with dim CBPs may decrease near the maximum of a sunspot cycle, thus supporting the explanation that the cycle variation of dim CBPs is due to the change in area of the solar disk occupied by a quiet Sun and the magnetic field of active regions. Similar to Sattarov *et al.* (2002), Figure 9 does not establish a causal relation between CBPs and magnetic bipoles. The question of a CBP–bipole association will be investigated separately.

**Figure 9** Cycle variation of number of magnetic bipoles with unsigned magnetic flux larger than 50 G.



## 5. Conclusions

In this study we use an automatic procedure to identify coronal bright points in EIT full disk images observed in the 195 Å spectral range. We find a slight decrease of the total number of CBPs near the maximum of the sunspot cycle. We have divided the CBPs into two categories based on their maximum brightness, and we found opposite trends in cycle variation of dim and bright CBPs. Dim CBPs, associated with a quiet Sun, vary inversely with sunspot cycle, while the variation of bright CBPs (active Sun CBPs) shows a positive correlation with sunspot cycle in agreement with previous studies. The latitudinal distribution of dim CBPs suggests their uniform distribution over the Sun, while bright CBPs show an enhancement at latitudes associated with sunspot activity belts. We approximate cycle variation of dim and bright CBPs by Gaussian functions. The sum of these two functions shows a modest 30% dip around the maximum of the sunspot cycle, thus supporting the notion of inverse variation of CBP number with sunspot cycle. Finally, we argue that the decrease in number of dim CBPs at a solar maximum is caused mainly by the reduction in area of mixed polarity quiet Sun fields (because the area occupied by active regions increases at the solar maximum). In our opinion, the visibility effect, when the bright corona obscures CBPs, plays only an auxiliary role.

**Acknowledgements** We thank Dr. J. Gurman for his advise on EIT CCD camera response and its correction. The National Solar Observatory is operated by the Association of Universities for Research in Astronomy (AURA Inc.) for the National Science Foundation. SOHO/EIT is the result of cooperation between NASA and ESA. NSO/Kitt Peak data used here are produced cooperatively by NSF/NOAO, NASA/GSFC, and NOAA/SEL. I. Sattarov and N. Karachik acknowledge partial support for this study from grant UZB-54(J) of Science and Technology Center in Ukraine. This study was partially supported by NASA's IAT NNH09AL04I. This research has made use of NASA's Astrophysics Data System Bibliographic Services. Figures 2 and 8 were included at the request of the anonymous referee.

## References

- Davis, J.M., Golub, L., Krieger, A.S.: 1977, *Astrophys. J.* **214**, L141.  
 Delaboudinière, J.-P., Artzner, G.E., Brunaud, J., Gabriel, A.H., Hochedez, J.F., Millier, F., *et al.*: 1995, *Solar Phys.* **162**, 291.  
 Giovanelli, R.G.: 1982, *Solar Phys.* **77**, 27.

- Golub, L., Davis, J.M., Krieger, A.S.: 1979, *Astrophys. J.* **229**, L145.
- Golub, L., Krieger, A.S., Vaiana, G.S.: 1975, *Solar Phys.* **42**, 131.
- Golub, L., Krieger, A.S., Vaiana, G.S.: 1976, *Solar Phys.* **50**, 311.
- Hara, H., Nakakubo-Morimoto, K.: 2000, *Adv. Space Res.* **25**, 1905N.
- Hara, H., Nakakubo-Morimoto, K.: 2003, *Astrophys. J.* **589**, 1062.
- Harvey-Angle, K.: 1993, 'Magnetic Bipoles on the Sun', Ph.D. Thesis, Utrecht University.
- Karachik, N., Pevtsov, A.A., Sattarov, I.: 2006, *Astrophys. J.* **642**, 562.
- Longcope, D.W., Kankelborg, C.C., Nelson, J.L., Pevtsov, A.A.: 2001, *Astrophys. J.* **553**, 429.
- McIntosh, S.W., Gurman, J.B.: 2005, *Solar Phys.* **228**, 285.
- Pevtsov, A.A., Acton, L.W.: 2001, *Astrophys. J.* **554**, 416.
- Sattarov, I., Pevtsov, A.A., Hojaev, A.S., Sherdonov, C.T.: 2002, *Astrophys. J.* **564**, 1042.
- Sattarov, I., Pevtsov, A.A., Karachik, N.V., Sherdanov, Ch.T.: 2005a, In: Stepanov, A.V., Benevolenskaya, E.E., Kosovichev, A.G. (eds.) *Multi-Wavelength Investigations of Solar Activity*, *IAU Symp.* **223**, 667.
- Sattarov, I., Pevtsov, A.A., Karachik, N.V., Tillaboev, A.M.: 2005b, In: Stepanov, A.V., Benevolenskaya, E.E., Kosovichev, A.G. (eds.) *Multi-Wavelength Investigations of Solar Activity*, *IAU Symp.* **223**, 665.
- Sattarov, I., Pevtsov, A.A., Karachik, N.V., Sattarova, B.J.: 2005c, In: Sankarasubramanian, K., Penn, M., Pevtsov, A. (eds.) *Large-Scale Structures and Their Role in Solar Activity*, *ASP Conf. Ser.* **346**, 363.
- Tlatov, A.G., Pevtsov, A.A., Singh, J.: 2009, *Solar Phys.* **255**, 239.
- Tsuneta, S., Acton, L., Bruner, M., Lemen, J., Brown, W., Carvalho, R., *et al.*: 1991, *Solar Phys.* **136**, 37.
- Webb, D.F., Martin, S.F., Moses, D., Harvey, J.W.: 1993, *Solar Phys.* **144**, 15.
- Zhang, J., Kundu, M.R., White, S.M.: 2001, *Solar Phys.* **198**, 347.